Empirical Plasmapause Model based on Swarm Observations

Balázs Heilig[1], **Hermann Lühr**[2]

1) Tihany Geophysical Observatory, Geological and Geophysical Institute of Hungary, Tihany, Hungary
2) GFZ German Research Centre for Geosciences, Telegrafenberg, 1473 Potsdam, Germany

Abstract Recently a new method for monitoring the plasmapause location in the equatorial plane was introduced by the authors based on magnetic field observations made by the CHAMP satellite in the topside ionosphere. Related signals are small-scale field-aligned currents (some 10km scale size) driven by interactions between the solar wind and the magnetosphere. Their equatorial boundary was found to be a good proxy for the location of the plasmapause. The method has been applied to the Swarm constellation of three identical satellites orbiting the Earth in the topside ionosphere on a polar orbit. Since the orbital period is around 90 minutes, the plasmapause is crossed around 60 times daily by each satellite. This makes this constellation very efficient in monitoring plasmapause dynamics. The boundary can be clearly found on the night side, especially during disturbed conditions, while on the day side the signals related to the plasmapause are often masked by other phenomena (e.g. ULF waves). These observations are validated and calibrated using the in-situ plasma density observations of the Van Allen Probes, and based on the calibrated values, a plasmapause model is constructed. The model, combined with recent Swarm observations, yield an estimate of the plasmapause location at any MLT.
.

Detection method

Our plasmapause (PP) model is based on the determination of the night side inner (equatorward) boundary of the occurrence of small-scale (some 10 km scale size) field-aligned currents (SSFACs). This boundary was found to correlate strongly with the location of the PP.

A **characteristic signal**, *S*, representing the SSFAC activity is derived through the following steps.:

1) Swarm single-satellite FAC density product is filtered using a 3rd order Butterworth high-pass filter with 250 mHz cutoff frequency (corresponds to 30 km wavelength).
2) the logarithm of the squared SSFAC density (in units of μAm^{-2}) is taken (Fig. 1, light blue line)
3) boxcar averaging over a 20 s window is applied to derive *S* (Fig. 1, dark blue line)

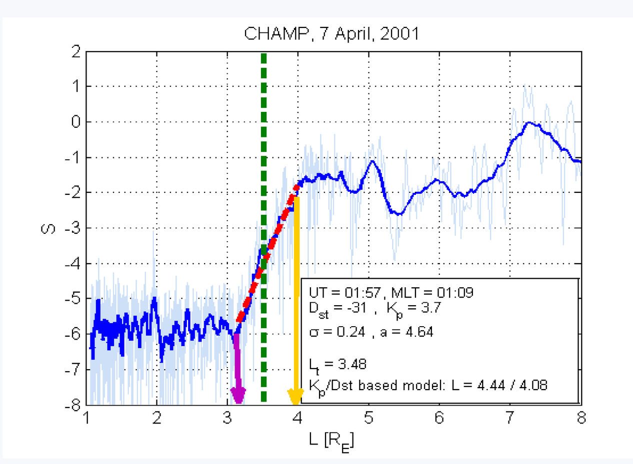

Fig. 1 Well-defined SSFAC boundary

Then orbit segments (from equator to pole) are scanned for **steep gradients**:

1) L_c, the lowest *L*-value (> 1.5) where *S* surpasses −2.5 (i.e. where $j_{\parallel} \approx 0.06$ μAm^{-2}), is determined (purple arrow in Fig. 1):

$$L_c = \min(L), \quad S(L) > -2.5, \quad L > 1.5$$

2) L_m, the highest *L*-value below L_c where *S* is less than −5.5 (i.e. where $j_{\parallel} \approx 0.002$ μAm^{-2}) is chosen (yellow arrow in Fig. 1):

$$L_m = \max(L), \quad S(L) < -5.5, \quad L < L_c$$

3) Linear fit to the curve *S* in the interval $[L_m; L_c]$ (red dashed line in Fig. 1)

$$S^*(L) = aL + b$$

4) L_{ssfac}, the transition point is calculated from the linear fit at $S^* = -4.1$ (green vertical dashed line in Fig. 1)

$$L_{ssfac} = (-4.1 - b)/a.$$

The reference value ($S^* = -4.1$) was chosen based on an analysis to find the best correlation between L_{ssfac}-values and the geomagnetic Kp index. In the following L_{ssfac} is referred to as the position of the (inner) SSFAC boundary, or simply the SSFAC index.

The boundary width dL is defined as $L_c - L_m$.

Correlation analysis (SSFAC index and Kp)

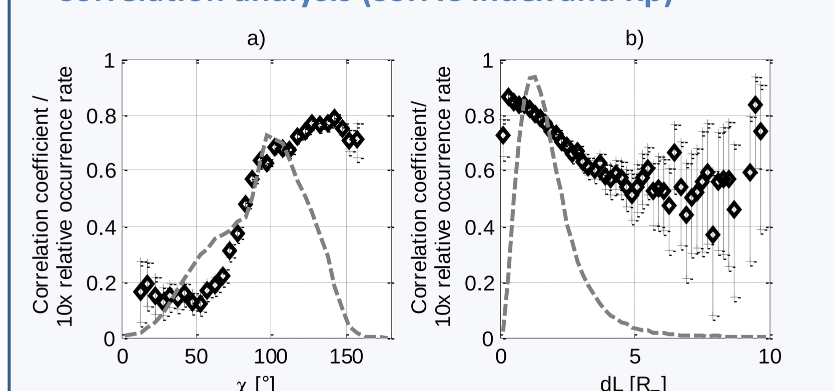

Fig. 2 Dependence of the correlation strength between the SSFAC index and the Kp index **(a)** on the solar zenith angle, χ, and **(d)** on the boundary width dL.

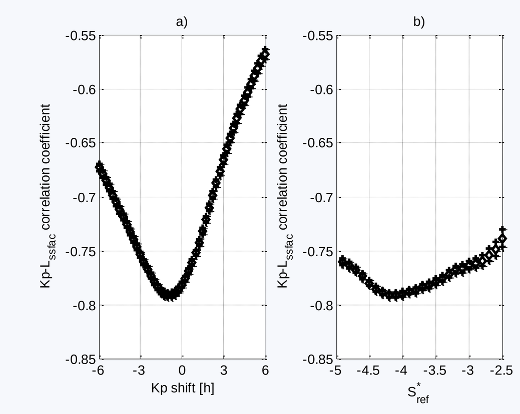

Fig. 3 Dependence of the correlation between the SSFAC index and the Kp index on **(a)** the time lag between the SSFAC index and Kp (cross-correlation), and **(b)** on the reference level chosen for *S** (used in the detection process).

Observations

1) The correlation is high night time (i.e. when $\chi > 90$, see Fig. 2 (a) and when dL, the width of the boundary is small, see Fig. 2 (b).
2) The correlation is the strongest at 1 hr time lag, see Fig. 3 (a).
3) The correlation is the strongest at the reference level $S^* = -4.1$, see Fig. 3 (b).

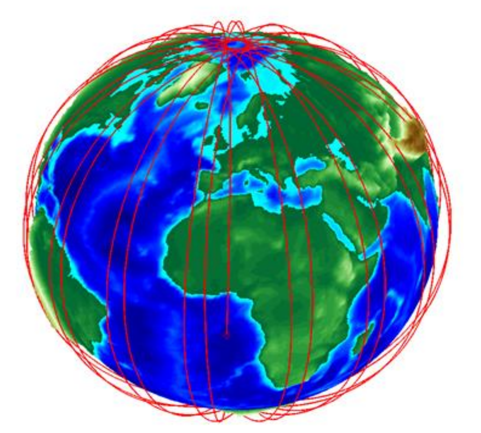

Fig. 4 Daily orbit of CHAMP/Swarm-like LEO s/c

Validation of the SSFAC index by in-situ NASA VAP PP crossings

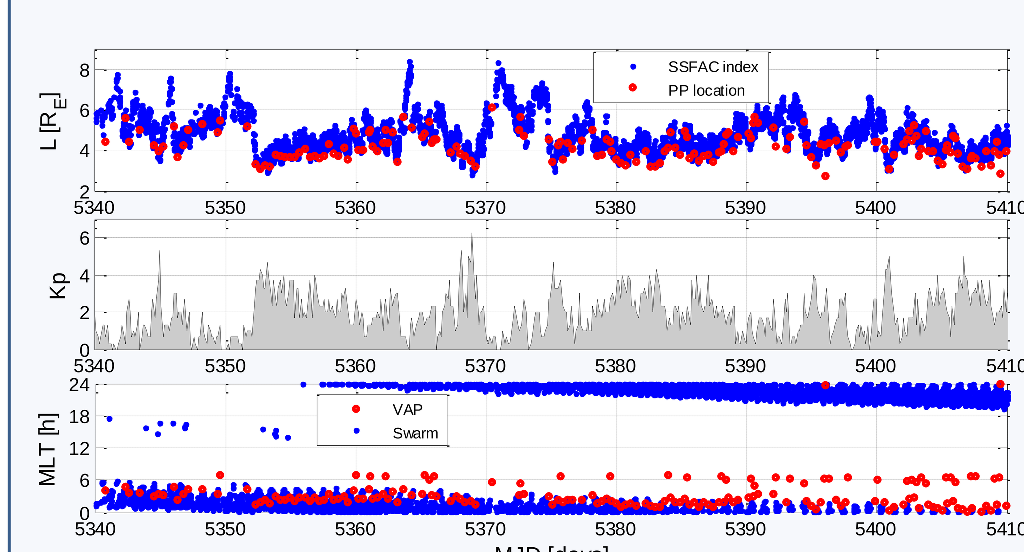

Fig. 7 (top) Swarm SSFAC index (blue) and VAP PP_Ne (red) locations, (middle) variation of the Kp index, (bottom) MLT of the Swarm (blue) and VAP (red) observations

Swarm SSFAC index

- **Over 68 000 Swarm** PP night side crossings were analysed (2014-2017)

VAP PP positions

- 1665 in-situ VAP PP crossings derived from VAP NURD e- density data.

Observations

1) SSFAC index yields an unprecedented detailed picture of PP dynamics (productivity)
2) SSFAC index can be derived automatically (potential for real-time service)

Empirical model of the SSFAC boundary

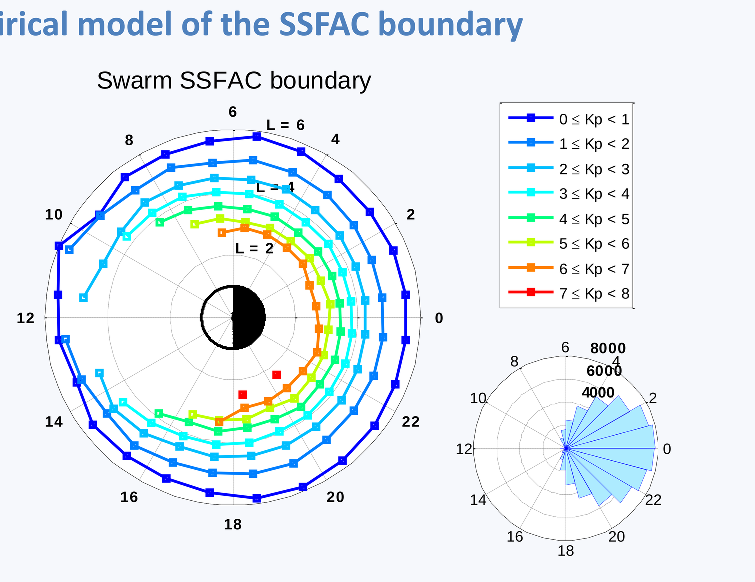

Fig. 5a MLT dependence of mean SSFAC index for different ranges of Kp (from outside inward Kp = 0–1, 1–2, 2–3, 3–4, 4–5, 5–6, 6–7, and 7-8, respectively). All Swarm data from 2014–2017 were used.

For a given Kp L_{ssfac} follows excentric circles on the dial plot (Fig. 5a). A simple SSFAC boundary model (Fig. 5b) dependent on Kp and MLT can be built. The position of a point *P* on the circle is given by its polar coordinates: L_{mod} and $\varphi = 2\pi \mathrm{MLT}/24$. If the circle is centred at $C(c, \varphi_c)$ and has a radius *R*, L_{mod} can be derived for any MLT by applying the formula:

$$L_{mod} = c \cdot \cos d\varphi + \sqrt{R^2 - c^2 \sin^2 d\varphi},$$

where $d\varphi = 2\pi\big((\mathrm{MLT} - \mathrm{MLT}_c)/24\big)$, and $\mathrm{MLT}_c = 24\,h * \varphi_c/360°$.

Moreover, we suppose, that the position of *C* and the radius of the circle, R have a linear/quadratic dependence on Kp, respectively, that is

$$R = R_0 + p_1\,\mathrm{Kp} + p_2\mathrm{Kp}^2,\ c = c_0 + \gamma_c \mathrm{Kp},\ \mathrm{MLT}_c = \mathrm{MLT}_0 + \gamma_{mlt}\mathrm{Kp},$$

where c_0 and MLT_0 define the position of the centre and R_0 is the radius of the circle both at Kp = 0, while $p_1, p_2, \gamma_c, \gamma_{mlt}$ are free model parameters. Based on 68344 boundary positions observed during the period 1 Jan, 2014 - 31 Dec, 2017, the following model parameters (with 95 % confidence bounds) were obtained:

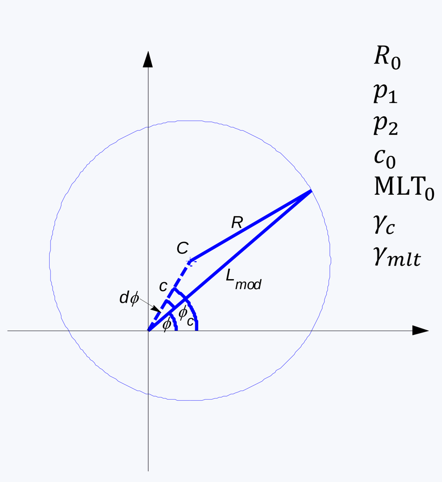

$$\begin{aligned} R_0 &= 6.12 \pm 0.07\ \mathrm{R_E}, \\ p_1 &= -0.709 \pm 0.03\ \mathrm{R_E}, \\ p_2 &= 0.0313 \pm 0.003\ \mathrm{R_E}, \\ c_0 &= 0.286 \pm 0.09\ \mathrm{R_E}, \\ \mathrm{MLT}_0 &= 12.24 \pm 0.79\ \mathrm{h}, \\ \gamma_c &= -0.031 \pm 0.018\ \mathrm{R_E}, \\ \gamma_{mlt} &= 0.193 \pm 0.31\ \mathrm{h}. \end{aligned}$$

Fig. 5b Sketch of the applied model for a fixed level of geomagnetic activity.

Fast response of the SSFAC boundary to changes in the geomagnetic activity

The variation of the boundary positions follow quite tightly any changes in Kp with an average response time of 0.5–1 hour (i.e. time difference or lag is between -0.5 and -1 h, Fig. 6). The interval length yielding the strongest correlation (deepest red) depends on the lag (positive lags are unphysical and can be attributed to the low (3 h) time resolution of Kp index). The absolute maximum is at -1 h lag and 0 h interval length, respectively, meaning that the night time SSFAC index is dependent mainly on the latest Kp index. Night time response of the SSFAC index to changes in Kp is practically immediate.

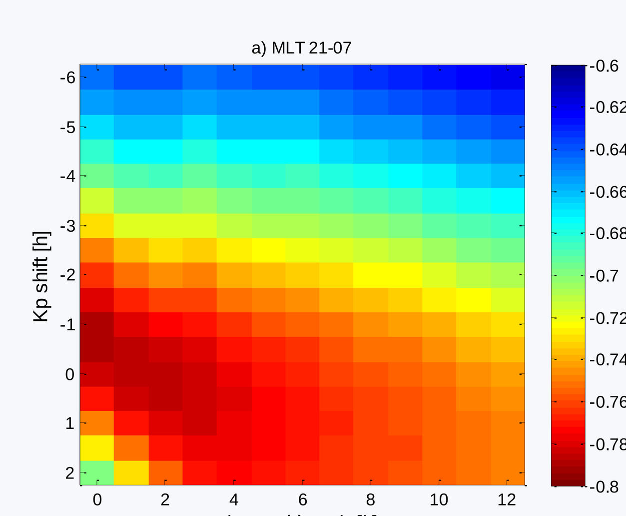

Fig. 6 Correlation strength between the SSFAC index and the peak Kp as a function of the length of the interval (horizontal axis), where the peak Kp is taken from the time difference (vertical axis) between the end of the interval and SSFAC index observation in the MLT sector 21- 07.

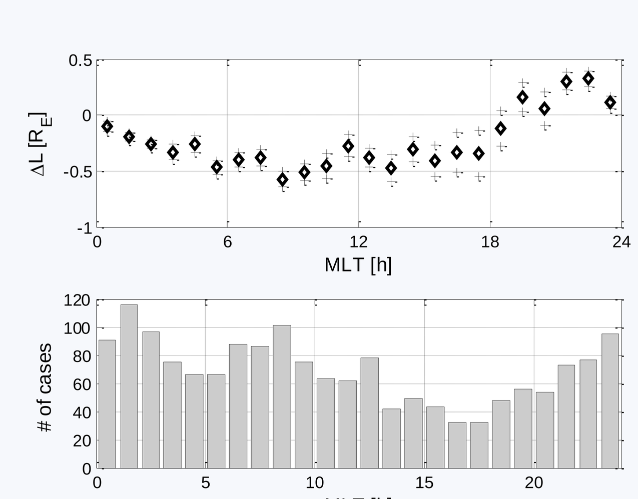

Fig. 8 : Mean difference between VAP PP position and Swarm SSFAC index as a function of MLT

We also estimated the mean separation between the boundaries as a function of MLT from 1665 Swarm crossings. SSFAC indices and simultaneous (UT difference is less than ±1 h) VAP PP positions were compared. The comparison (Fig. 8) revealed a clear bulge signature in the pre-midnight sector (19-01 h MLT) peaking at 21-22 h MLT. Elsewhere the SSFAC boundary is found typically poleward of the PP by ~0.2 R.

Cross-correlation between Swarm SSFAC boundary and in-situ VAP PP locations

The plasmasphere is well-known to have a dusk-side bulge and its distance at different MLTs can be quite different, controlled by the past variation of magnetospheric convection. On the contrary, the SSFAC boundary responds almost simultaneously at all MLTs (within about an hour) to changing conditions. The two boundaries are coupled only near midnight and in the early morning sector.

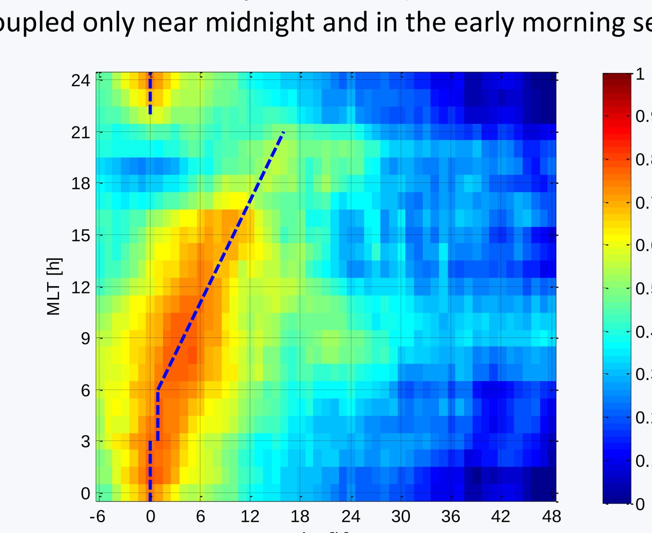

Fig. 9 : Cross-correlation between VAP PP position and the SSFAC index as a function of MLT

This difference and link between the two boundaries was confirmed by a cross-correlation analysis. Between 21-06 the cross correlation peaks at 0 h time lag, i.e. the variation of the boundaries is simultaneous. By contrast, on the dayside the PP location depends on past SSFAC indices. We can conclude that the new PP is formed on the night side, and propagates to the dayside by the co-rotation of the plasma with the Earth. The minimum correlation around 17 MLT is a consequence of the dusk-side bulge that is a feature of the PP, but not that of the SSFAC boundary.

Conclusions

1) The night side inner boundary of small-scale field-aligned currents (SSFACs) is closely related/located to the location of the plasmapause (PP) at all levels of geomagnetic activity. The SSFAC boundary cannot be determined reliably on the dayside (08:00 to 16:00MLT) and during extended quiet periods.
2) There is a strong control of the SSFAC radial distance by the geomagnetic activity indices Kp , Dst and AE.
3) The night side PP is generally found earthward of SSFACs, on average by about 0.2 R_E, except for the dusk side bulge region.
4) .While the PP shape, due to its co-rotation with Earth and the localized erosion, is determined by the Kp evolution in the preceding days, the SSFAC index responses within a few hours simultaneously at all MLTs. This difference has important implications for the derivation of a future PP model that is based on SSFAC boundary detections..

References

Heilig B., and Lühr, H. (2013): New plasmapause model derived from CHAMP field-aligned current signatures, *Ann. Geophys.*, *31*, 1-11.

Heilig, B. and Lühr, H. (2018): Quantifying the relationship between the plasmapause and the inner boundary of small-scale field-aligned currents, as deduced from Swarm observations, *Ann. Geophys.*, *36*, 595-607.

Acknowledgements

We are grateful to Yuri Shprits for fruitful scientific discussions and for providing the VAP NURD electron density dataset. We thank ESA for providing Swarm Level 1b magnetic field data through project SSVO 2011 no. 10242 (PI V BH) and for Swarm Level 2 product FACxTMS_2F.We acknowledge the use of the NASA/GSFC's Space Physics Data Facility's ftp service providing OMNI data. Balázs Heilig is funded by the Government of Hungary through an ESA contract under PECS (Plan for European Cooperating States) no. 4000114839/15/NL/NDe and the Bolyai Scholarship of the Hungarian Academy of Sciences. This study was performed as part of ESA-funded project "P2-SWE-XVI –Swarm Utilization Analysis" contract no. 4000117636/16/D/MRP and by DFG Priority Programme "DynamicEarth", SPP-1788.